

1 **THE ROLE OF PARTICLE SHAPE ON THE HYDRAULIC CONDUCTIVITY OF**
2 **GRANULAR SOILS CAPTURED THROUGH KOZENY-CARMAN APPROACH**

3 **Thanh Trung Nguyen and Buddhima Indraratna**

4 *Nguyen, T.T. and Indraratna, B. 2020. The role of particle shape on the hydraulic*
5 *conductivity of granular soils captured through Kozeny-Carman approach. Géotechnique*
6 *Letters, 10(3): 1-15. doi: 10.1680/jgele.20.00032.*

7 **Abstract**

8 Previous studies indicate that particle shape plays an important role in the hydraulic
9 conductivity (k) of granular materials, often represented through the Kozeny-Carman (KC)
10 concept. Several recent studies have improved the accuracy of the KC approach using the
11 particle size distribution (PSD) to estimate the specific surface area of particles but overly
12 simplifying the effect of particle shape. This current study innovatively adopts the Micro-
13 Computed Tomography (CT) technique to compute particle shape parameters of different
14 granular materials (e.g., glass beads, sand and crushed gravel) and then incorporate these
15 parameters into the KC equation to estimate k more accurately, which is then validated with
16 experimental data. The results indicate that k varies significantly according to different
17 particle shapes even if the same mean porosity and PSD are retained. Particles that are less
18 spherical and rounded have a larger fluid-particle contact area (i.e., larger shape factor),
19 hence a smaller hydraulic conductivity. The study suggests a shape factor of 1.28–1.52 for
20 natural sand and 1.84–2.1 for crushed sand and gravel can be used for KC method to estimate
21 k while a porosity-dependent equation is proposed to estimate the tortuosity for different
22 shaped materials.

23
24 *Keywords:* Microscopy; Permeability; Sands

25 **List of notation**

26	A_o	specific surface area of particles
27	$A_{o,s}$	specific surface area of spherical particles
28	$A_{o,i}$	specific surface area of irregular particles
29	A_p	cross-sectional area of particle
30	AG	angularity of particles
31	AR	aspect ratio of particles
32	k	hydraulic conductivity
33	n	porosity
34	p_{mi}	probability of particle size d_i
35	P_p	perimeter of particle
36	S_p	surface area of particle
37	S	sphericity of particles
38	τ	tortuosity of the flow
39	V_p	Volume of particle
40	α	shape factor
41	γ	unit weight of fluid
42	μ	dynamic viscosity of fluid
43	σ_v	coefficient of variation

44 Introduction

45 The effect that the micro-characteristics of particles have on the hydraulic behaviour of
46 geomaterials has received considerable attention, especially in recent years thanks to
47 advanced micro-scanning and computational methods (Matyka et al. 2008; Zhou and Wang
48 2015; Nguyen and Indraratna 2017a). Although computer-based approaches have indicated
49 certain advantages in predicting the hydraulic behaviour of porous geomaterials, empirical
50 methods such as Kozeny-Carman (KC) are still used widely in practice due to their simplicity
51 (Chapuis and Aubertin 2003; Zheng and Tannant 2017; Feng et al. 2019). The KC method
52 uses the fundamental parameters of a porous medium such as the specific surface area of
53 solid particles (A_o), the porosity (n) and the tortuosity (τ) to estimate the hydraulic
54 conductivity (k), which can be represented by (Trani and Indraratna 2010):

$$k(m/s) = \frac{1}{2\tau} \frac{\gamma}{\mu} \frac{1}{A_o^2} \frac{n^3}{(1-n)^2} \quad [1]$$

55 where γ and μ are the unit weight and dynamic viscosity of the fluid.

56 The main problem with this solution is how to determine A_o accurately. Previous
57 studies (Trani and Indraratna 2010; Ozgumus et al. 2014; Zheng and Tannant 2017) have
58 considered an equivalent uniform particulate medium, however, A_o can actually be
59 determined directly from the particle size distribution (PSD) of soil. Basically, A_o is defined
60 as the ratio between the total surface area $\sum S_i$ and the total volume $\sum V_i$ of particles in a
61 medium, so given the PSD of a perfectly spherical assembly, the value of A_o (i.e., $A_{o,s}$) can
62 be estimated by:

$$A_{o,s} = 6 \sum \frac{p_{mi}}{d_i} \quad [2]$$

63 where p_{mi} is the probability of particle size d_i occurring. Since most granular materials used
64 for geoenineering purposes are irregular in shape, the actual value of A_o (i.e., $A_{o,i}$) deviates

65 from $A_{o,s}$; thus the shape factor α is needed to consider this difference, i.e.,

$$A_{o,i}^2 = \alpha A_{o,s}^2 \quad [3]$$

66 Clearly, α approaches 1 when the particles are more spherical. In many versions of the KC
67 method, α and τ can be combined into the empirical Kozeny constant k_k (Ozgumus et al.
68 2014; Nguyen and Indraratna 2017b).

69 Trani and Indraratna (2010) improved the KC method by using the surface area
70 distribution (PSDsa) instead of conventional particle size distribution based on mass (PSDm),
71 however, α , τ and k_k have not been addressed properly. While considerable effort (Matyka et
72 al. 2008; Ozgumus et al. 2014; Zheng and Tannant 2017) has gone into evaluating these
73 parameters, there is still a lack of experimental methods to quantify them accurately. The
74 current study therefor uses a high resolution Micro-Computed Tomography (Micro-CT)
75 scanning followed by image processing to compute micro-parameters such as the surface area
76 and volume of soil particles that are then used to estimate the KC parameters (i.e., $A_{o,i}$ and the
77 associated α). Hydraulic conductivity tests of selected soils are also carried out to validate the
78 KC method.

79 **Experimental investigation into the effect of particle shape on hydraulic conductivity**

80 *Soil samples*

81 In this study, coarse sand (CS) and crushed gravel (CG) were used in comparison to artificial
82 glass beads (GB). While the PSDm of these soils was almost the same (i.e., the uniformity
83 coefficient $C_u = 1.4$), they had different shapes that could distinctly affect their hydraulic
84 conductivity. Two other natural soils, i.e., medium (MS) and fine (FS) sand with C_u of 1.6
85 and 2.1, respectively were also used. The PSD of these soils (measured by Mastersizer 3000
86 based on laser diffraction technique) is shown in Fig. 1 where they are compared with

87 granular materials used in previous studies. Optical microscopic view (Fig. 2a) shows that the
88 CG particles are very angular, whereas CS particles are more rounded while the GB particles
89 are almost perfectly spherical. Particles of MS are of similar shape to that of CS, whereas
90 particles of FS are more angular.

91 *Micro-CT scanning and laboratory procedure*

92 Micro-CT scanning is a cost effective method of capturing the geometric properties of porous
93 materials (Zhou and Wang 2015; Zhou et al. 2018; Nguyen and Indraratna 2019), so it was
94 used to determine the micro-geometric parameters of soil in this study. An X-ray scanner
95 (Sky-Scanner model 1275) which could produce images of the sample to a resolution of $4\ \mu\text{m}$
96 to ensure an acceptable accuracy (i.e., $< 3\%$ difference in the computed area compared to
97 optical scanning for the current materials) was employed (Nguyen et al. 2020). The sample
98 (in loose states by pouring particles into a container) was scanned every 0.1° to achieve
99 accurate 3 dimensional (3D) geometric characteristics. Imaging techniques including
100 filtering, binarizing, de-speckling, and watershed (i.e., for separating particles in contact)
101 were applied to the CT images to enhance the computational accuracy (Nguyen and
102 Indraratna 2019). The final process is a 3D analysis of the sample to capture the geometric
103 parameters of particles; this image processing took place using CTan.1.18 software (Brucker-
104 microCT 2018). Specifically, the surface area and volume of particles were computed so that
105 their $A_{o,i}$ and the associated α could then be obtained (i.e., Eq. [3]).

106 Some of the fundamental geometric parameters that are commonly used to evaluate
107 the shape properties of particles can be estimated using CT scanning images. Table 1 shows
108 the detailed equations and their corresponding results of sphericity S (i.e., represents how
109 close the particle geometry is to a sphere), the aspect ratio AR (i.e., the ratio between the
110 major and minor axes of a particle) and the angularity AG (the degree of sharpness of particle

111 corners and edges) (Cho et al. 2006). Fig. 2b shows 3D samples reconstructed from Micro-
112 CT scanning images, which indicates a high accuracy of the technique in computing particle
113 shape characteristics.

114 A series of laboratory tests based on ASTM D2423 (2005) were carried out to
115 determine the hydraulic conductivity (k) of the current samples. Each sample was first poured
116 into the cell in a loose state to which different levels of compaction (i.e., tamping by layer)
117 were then applied to achieve different degrees of packing, but over-compaction was avoided
118 to prevent undue degradation (i.e, scanning specimen after compaction before hydraulic test
119 to identify the limit of compaction). Measurement was repeated at each specimen and
120 porosity to ensure the reliable results (i.e., the coefficient of variation $< 1\%$).

121 **Results and Discussion**

122 *Quantitative characteristics of particle shape*

123 Table 1 shows that GB has the largest sphericity ($S = 0.95$), followed by CS ($S = 0.73$) and
124 CG ($S = 0.5$). The AR of CS is about 1.49 which is much larger than GB ($AR = 1.06$), but this
125 is still smaller than CG (i.e., 2.45). Undoubtedly, the CG particles are very angular because
126 their average angularity is only about 0.27 which is much smaller than that of CS (0.57) and
127 GB (0.98). As a result, CG has the largest α (2.1), followed by CS (1.45) and GB (1.02). In
128 essence, the more angular and less spherical, the larger is the surface area per a unit particle
129 volume (i.e., the larger the α). Moreover, the geometric parameters are dispersed more
130 widely (i.e., the larger the coefficient of variation c_v) when the particles are less spherical. For
131 instance, the c_v of angularity increases from 15.5% in CS to 34.9% in CG.

132 *Hydraulic conductivity of different materials*

133 Fig. 3 shows the hydraulic test results where k varies with n over different materials (medium

134 to loose state). Apparently, GB has the largest k (8.1×10^{-3} m/s) followed by CS with $k =$
135 4.3×10^{-3} m/s at the same porosity, i.e., $n = 0.39$. The CG particles are more angular and less
136 spherical, thus they have a much lower k , i.e., 2.0×10^{-3} m/s at the same porosity. Unlike CS,
137 MS and FS with larger specific surface areas as shown in Table 1 (i.e., the fluid-particle
138 contact area) give a much smaller value of k , for example about 1.0×10^{-3} m/s and 5.2×10^{-4}
139 m/s, respectively at $n = 0.39$.

140 *Evaluating the shape factor in the Kozeny-Carman (KC) approach*

141 Using the value of $A_{o,i}$ shown in Table 1, the hydraulic conductivity of the current soils can
142 be estimated by Eq. [1]. The tortuosity (τ) generally varies with porosity (n), which can be
143 represented by (Comiti and Renaud 1989)

$$\tau = 1 - p \ln(n) \quad [4]$$

144 where p is an empirical parameter varying with different materials. By comparing the
145 predicted and experimental results, $p = 0.6$, 1.15 and 2.4 were found to provide reasonable
146 predictions for 3 different distinct levels of particle shape parameters, i.e., glass beads, sand
147 and crushed gravel, respectively. As a result, Fig. 3a shows an accurate prediction with the
148 average error less than 4% across all specimens. Without properly determining α , the
149 predicted k could deviate considerably, for example, from 8.1×10^{-3} in GB to 2.0×10^{-3} in CG
150 despite using the same PSD and porosity ($n = 0.39$). In other words, the current study has
151 corrected the previous limitations (e.g., Trani and Indraratna 2010) where the role of α is
152 ignored while computing k .

153 Fig. 3b is an application of the current findings to other granular soils such as Ottawa,
154 Toyoura, Nevada and crushed sand which have commonly been used in previous studies (Lin
155 2006; Kokusho and Fujikura 2008; Cote et al. 2011; Fleshman and Rice 2014). Without
156 knowing the specific shape parameters and an accurate method to measure τ of these

157 materials, it might be assumed that other natural (uncrushed) sands should be similar in
158 particle shape compared to the current sands while particles of crushed sands would be highly
159 angular (Cote et al. 2011). Therefore, the same values of p , i.e., 1.15 and 2.4 for natural and
160 crushed sands, respectively can be assumed to estimate τ while α is varied in a range (i.e.,
161 1.28 to 1.51) that is close to the current findings for natural sands, and 1.84 for crushed sand.
162 Note that $A_{o,s}$ of these soils is computed by Eq. [2] based on their PSD curves (Fig. 1). The
163 results (Fig. 3b) show that the current KC prediction matches relatively well the experimental
164 data, i.e., the average error in prediction across different soils about 5.7%. Despite this
165 success, a detailed computation of α for specific materials based on micro-CT scanning is
166 still recommended to further enhance accuracy of the predicted k .

167 *Behaviour of the flow tortuosity (τ)*

168 A back-analysis of τ (Fig. 4) based on experimental data ($A_{o,i}$ and k) shows 3 distinct levels of
169 τ corresponding to different levels of particle shape parameters (glass beads, sand and
170 crushed gravel). In essence, the more compacted the particles (i.e., the smaller the n), the
171 more complex the resulting seepage flow; and the less spherical and rounded the particles, the
172 greater the tortuosity. The current estimate $\tau = 1 - 1.15\ln(n)$ for sandy soils shows better
173 agreement with experimental data than previous models, i.e., Comiti and Renaud (1989), and
174 Iversen and Jorgensen (1993) while $\tau = 1 - 0.6\ln(n)$ for glass beads is relatively close to
175 the theoretical derivation of Weissberg (1963) for overlapping spheres. However, $p = 2.4$ for
176 crushed materials indicates a lower degree of agreement with experimental data where the
177 particles might rearrange themselves due to compaction. Thus an alternative relationship, i.e.,
178 $\tau = 1 + 3.55(1 - n)$ is proposed to improve the accuracy. As a result from the current study,
179 the Kozeny constant k_k (i.e., $k_k = 2\alpha\tau$) can then be established as about 5.1–6.8 for natural
180 sands, and 10.9–13.6 for crushed materials for future KC applications.

181 **Conclusion**

182 This study explained how particle shape could influence the hydraulic conductivity (k) of
183 granular soils, and then reinvigorating the Kozeny-Carman method using Micro-CT data. The
184 results showed that particle shape would play an important role in the hydraulic conductivity
185 of granular materials, thus the less spherical and rounded the grain shape, the larger would be
186 the fluid-particle contact area (i.e., the larger the shape factor α), and therefore, the lower the
187 k . Crushed gravel had an α that is 2.1 times larger than that of corresponding glass beads,
188 making its hydraulic conductivity 4.0 times lower, despite having the same n (0.39) and PSD.
189 This study recommended an α of about 1.28–1.52 for natural (uncrushed) sand and 1.84–2.1
190 for crushed materials can be adopted when using KC concept to predict k . Also in this regard,
191 the tortuosity estimate $\tau = 1 - p \ln(n)$ where $p = 0.6$ and 1.15 for spheres and natural sand,
192 respectively, and $\tau = 1 + 3.55(1-n)$ for crushed materials can be suggested for computing k .

193

194 **Acknowledgements**

195 This research was supported by the Australian Government through the Australian Research
196 Council's Linkage Projects funding scheme (LP160101254), and the Industrial
197 Transformation Training Centre for Advanced Technologies in Rail Track Infrastructure
198 (ITTC-Rail), University of Wollongong. The financial and technical support from SMEC,
199 Coffey, GeoHabour-Australia, Sydney Trains and ARTC (Australian Rail Track Corporation)
200 is much appreciated.

201

References

- ASTM D2432-68. 2005. Standard test method for permeability of granular soils (constant head). American Society for Testing and Materials, West Conshohocken, Pa.
- Brucker-microCT. 2018. Manual for Bruker-microCT CT-analyser V.1.18.
- Chapuis, R.P. and Aubertin, M. 2003. On the use of the Kozeny– Carman equation to predict the hydraulic conductivity of soils. *Canadian Geotechnical Journal*, **40**(3): 616-628. doi: 10.1139/t03-013.
- Cho, G.-C., Dodds, J. and Santamarina, J.C. 2006. Particle shape effects on packing density, stiffness, and strength: natural and crushed sands. *Journal of Geotechnical and Geoenvironmental Engineering*, **132**(5): 591-602. doi: doi:10.1061/(ASCE)1090-0241(2006)132:5(591).
- Comiti, J. and Renaud, M. 1989. A new model for determining mean structure parameters of fixed beds from pressure drop measurements: application to beds packed with parallelepipedal particles. *Chemical Engineering Science*, **44**(7): 1539-1545. doi: [https://doi.org/10.1016/0009-2509\(89\)80031-4](https://doi.org/10.1016/0009-2509(89)80031-4).
- Cote, J., Fillion, M.-H. and Konrad, J.-M. 2011. Estimating Hydraulic and Thermal Conductivities of Crushed Granite Using Porosity and Equivalent Particle Size. *Journal of Geotechnical and Geoenvironmental Engineering*, **137**(9): 834-842. doi: doi:10.1061/(ASCE)GT.1943-5606.0000503.
- Feng, S., Vardanega, P.J., Ibraim, E., Widyatmoko, I. and Ojum, C. 2019. Permeability assessment of some granular mixtures. *Géotechnique*, **69**(7): 646-654. doi: 10.1680/jgeot.17.T.039.
- Fleshman, M.S. and Rice, J.D. 2014. Laboratory modeling of the mechanisms of piping erosion initiation. *Journal of Geotechnical & Geoenvironmental Engineering*, **140**(6):

04014017:1-12.

- Iversen, N. and Jørgensen, B.B. 1993. Diffusion coefficients of sulfate and methane in marine sediments: Influence of porosity. *Geochimica et Cosmochimica Acta*, **57**(3): 571-578. doi: [https://doi.org/10.1016/0016-7037\(93\)90368-7](https://doi.org/10.1016/0016-7037(93)90368-7).
- Kokusho, T. and Fujikura, Y. 2008. Effect of particle gradation on seepage failure in granular soils. *In Proceedings of the 4th International Conference on Scour and Erosion (ICSE-4)*, 5-7, November, Tokyo, Japan. pp. 497-504.
- Lin, Y. 2006. Colloidal silica transport mechanics for passive site stabilization of liquefiable soils. Doctor of Philosophy. thesis, Drexel University
- Matyka, M., Khalili, A. and Koza, Z. 2008. Tortuosity-porosity relation in porous media flow. *Physical Review E*, **78**(2): 026306. doi: 10.1103/PhysRevE.78.026306.
- Nguyen, T.T. and Indraratna, B. 2017a. Experimental and numerical investigations into hydraulic behaviour of coir fibre drain. *Canadian Geotechnical Journal*, **54**(1): 75-87. doi: 10.1139/cgj-2016-0182.
- Nguyen, T.T. and Indraratna, B. 2017b. The permeability of natural fibre drains, capturing their micro-features. *Proceedings of the Institution of Civil Engineers - Ground Improvement*, **170**(3): 123-136. doi: 10.1680/jgrim.16.00032.
- Nguyen, T.T. and Indraratna, B. 2019. Micro-CT scanning to examine soil clogging behavior of natural fiber drains. *Journal of Geotechnical and Geoenvironmental Engineering*, **145**(9): 04019037. doi: 10.1061/(ASCE)GT.1943-5606.0002065.
- Nguyen, T.T., Indraratna, B. and Baral, P. 2020. Biodegradable prefabricated vertical drains: from laboratory to field studies. *Geotechnical Engineering Journal of the SEAGS & AGSSEA*, **51**(2): 39-46.
- Ozgunus, T., Mobedi, M. and Ozkol, U. 2014. Determination of kozeny constant based on porosity and pore to throat size ratio in porous medium with rectangular rods.

- Engineering Applications of Computational Fluid Mechanics, **8**(2): 308-318.
- Trani, L.D.O. and Indraratna, B. 2010. The use of particle size distribution by surface area method in predicting the saturated hydraulic conductivity of graded granular soils. *Géotechnique*, **60**(12): 957-962. doi: 10.1680/geot.9.T.014.
- Weissberg, H.L. 1963. Effective diffusion coefficient in porous media. *Journal of Applied Physics*, **34**(9): 2636-2639. doi: <https://doi.org/10.1063/1.1729783>.
- Zheng, W. and Tannant, D.D. 2017. Improved estimate of the effective diameter for use in the Kozeny–Carman equation for permeability prediction. *Géotechnique Letters*, **7**(1): 1-5. doi: 10.1680/jgele.16.00088.
- Zhou, B. and Wang, J. 2015. Random generation of natural sand assembly using micro x-ray tomography and spherical harmonics. *Géotechnique Letters*, **5**(1): 6-11. doi: 10.1680/geolett.14.00082.
- Zhou, B., Wang, J. and Wang, H. 2018. Three-dimensional sphericity, roundness and fractal dimension of sand particles. *Géotechnique*, **68**(1): 18-30. doi: 10.1680/jgeot.16.P.207.

Tables

No	Material	Specific gravity (G_s)	Uniformity coefficient (C_u)	Sphericity ($S = \frac{4\pi A_p}{P_p^2}$)	Aspect ratio (ratio between the major and minor axes)	Angularity ($AG = \frac{\sum r_i/n_c}{r_{max}}$)	$A_{o,s}$ ($\Sigma S_i/\Sigma V_i$) (based on PSD) (1/m)	$A_{o,i}$ ($\Sigma S_i/\Sigma V_i$) (CT-scanning) (1/m)	Shape factor ($\alpha = A_{o,i}^2/A_{o,s}^2$)
1	Glass beads (GB)	2.46	1.4	0.95 ($c_v = 5.0\%$)	1.06 ($c_v = 11.5\%$)	0.98 ($c_v = 5.1\%$)	7812	7892.0	1.02
2	Coarse sand (CS)	2.65	1.4	0.73 ($c_v = 12.3\%$)	1.49 ($c_v = 21.6\%$)	0.57 ($c_v = 15.5\%$)	7809	9410	1.45
3	Crushed gravel (CG)	2.58	1.4	0.50 ($c_v = 25\%$)	2.45 ($c_v = 46.7\%$)	0.27 ($c_v = 34.9\%$)	7829	11352	2.10
4	Medium sand (MS)	2.68	1.6	0.74 ($c_v = 11.5\%$)	1.53 ($c_v = 24.5\%$)	0.56 ($c_v = 21.8\%$)	15921	19328	1.47
5	Fine sand (FS)	2.67	2.1	0.705 ($c_v = 14.4\%$)	1.63 ($c_v = 32.5\%$)	0.48 ($c_v = 22.5\%$)	22073	27260	1.52

Note: c_v is the coefficient of variation (%); A_p and P_p are the area and perimeter of particle's cross-section; r_i and r_{max} are the radii of the corner and the maximum inscribed circle of the particle, and n_c is the number of corners in the particle. More details can be found in Cho et al. (2006)

Table 1 Micro-parameters of granular soils used in the current study

List of figures

Fig. 1 Particle size distribution of soils used in this study.....	15
Fig. 2 Micro-scanning techniques: a) optical microscopic observation; b) 3D reconstruction under Micro-CT scanning.....	16
Fig. 3 Hydraulic conductivity of different materials by experimental and KC methods: a) current study; b) compared to previous granular soils.....	18
Fig. 4 Tortuosity of fluid flow through different shaped materials in comparison with previous studies.....	19

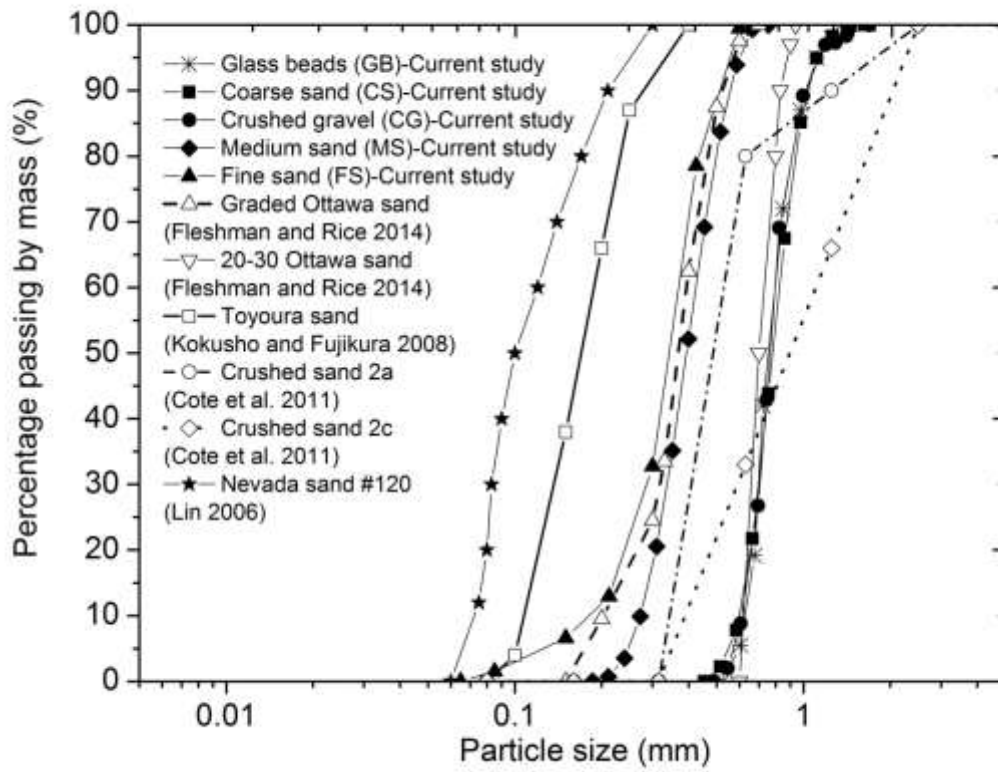
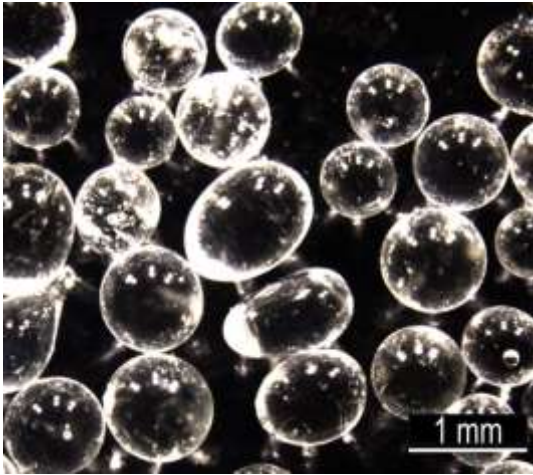
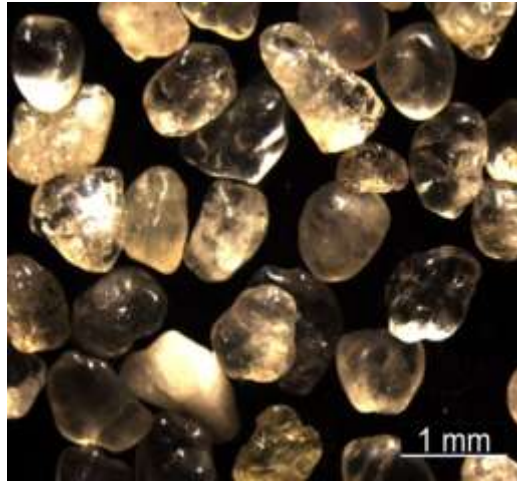


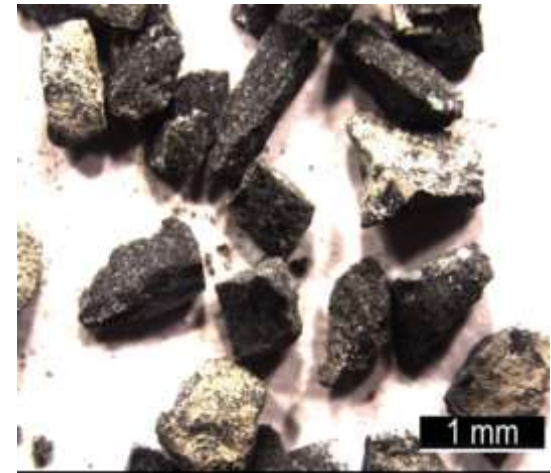
Fig. 1 Particle size distribution of soils used in this study



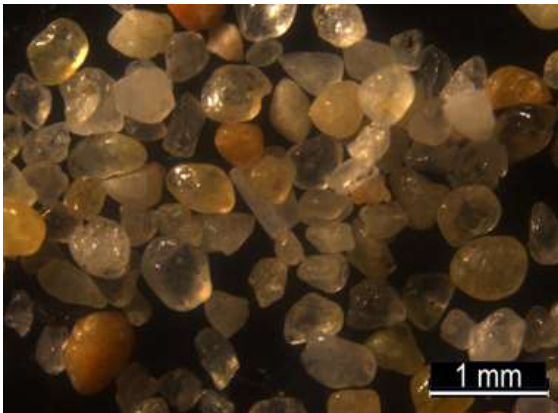
Glass beads (GB)



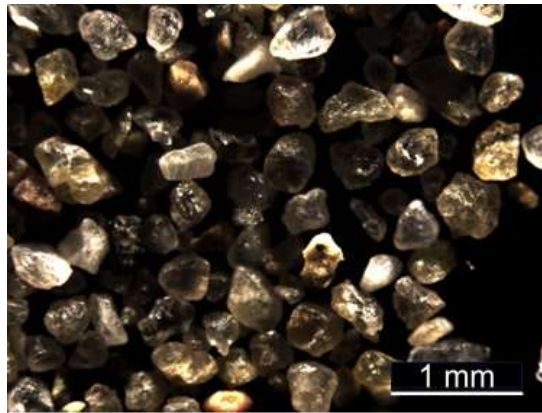
Coarse sand (CS)



Crushed gravel (CG)



Medium sand (MS)



Fine sand (FS)

a)

Fig. 2 Micro-scanning techniques: a) optical microscopic observation; b) 3D reconstruction under Micro-CT scanning

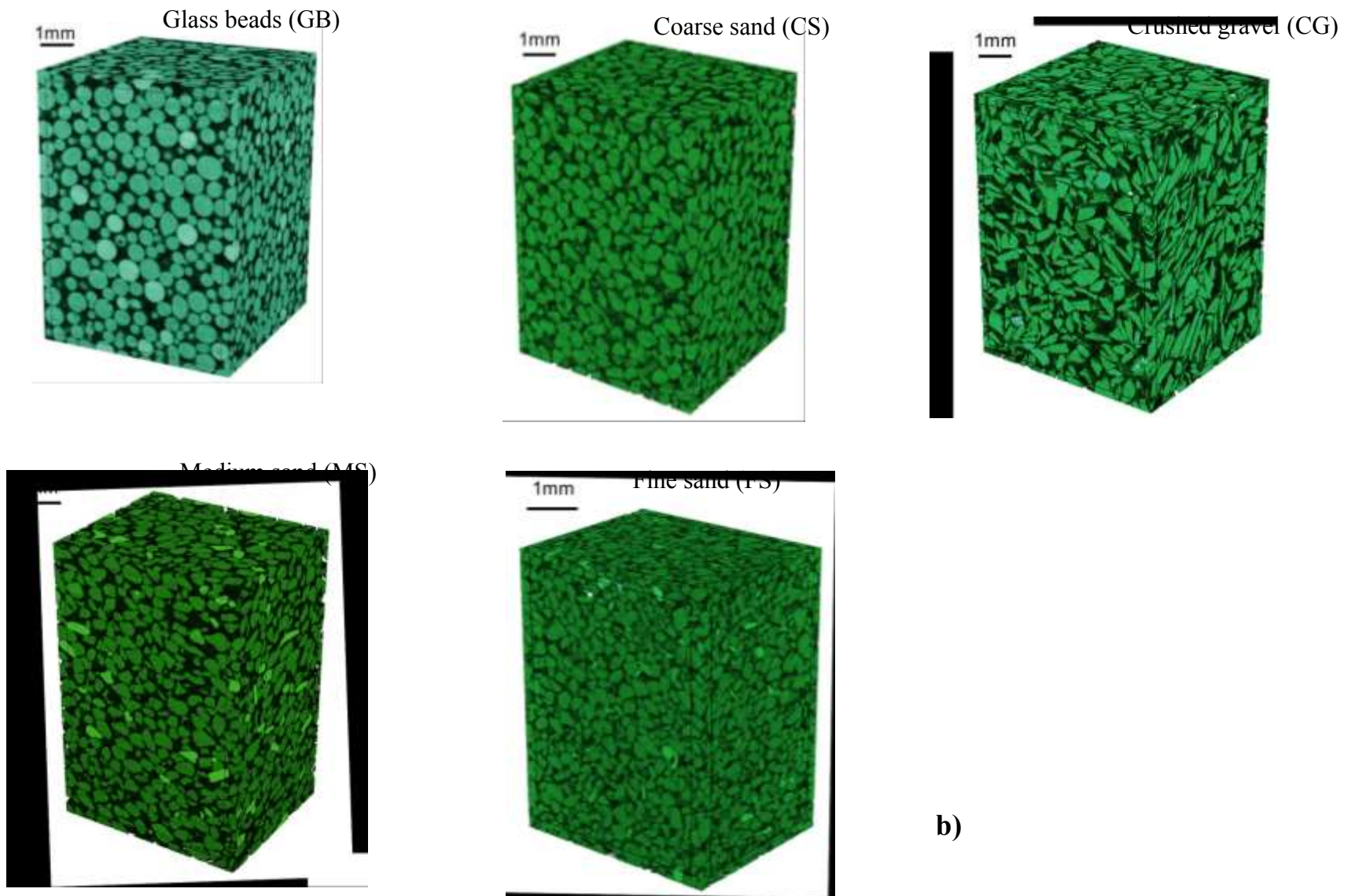
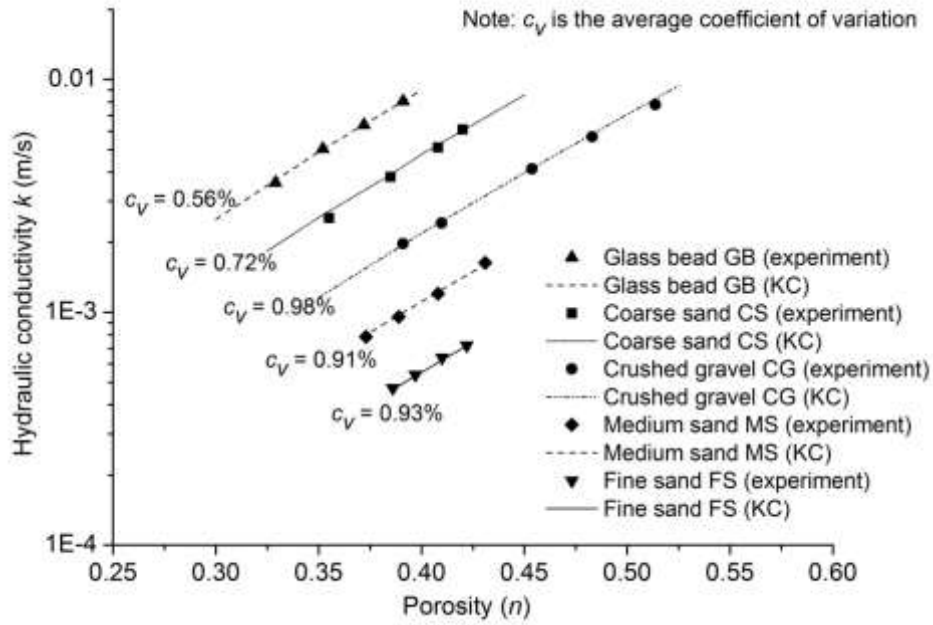
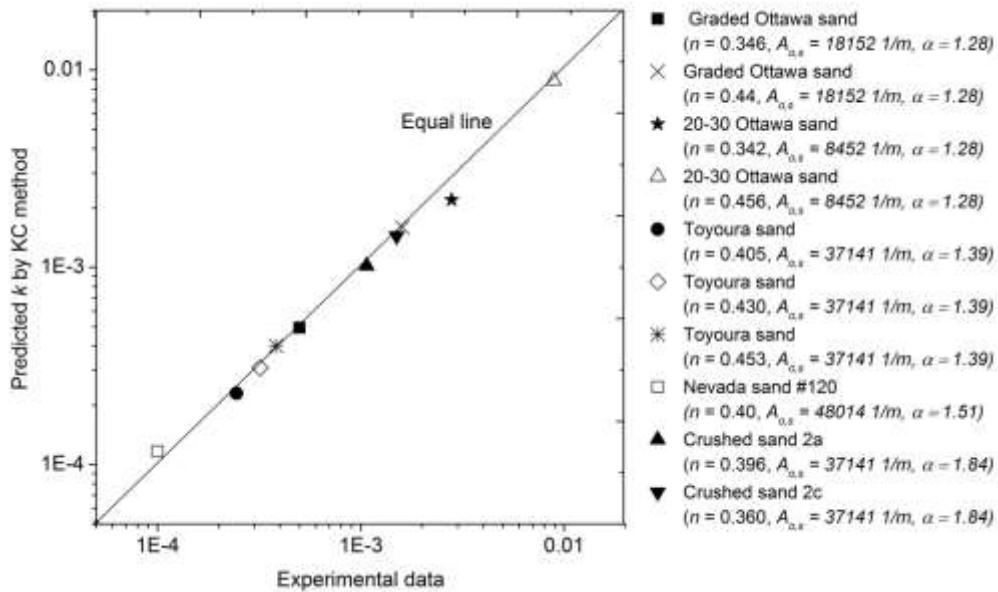


Fig. 2 Micro-scanning techniques: a) optical microscopic observation; b) 3D reconstruction under Micro-CT scanning (**continued**)



a)



b)

Note: The experimental data are taken from following studies: Nevada sand (Lin 2006); Toyoura sand (Kokusho and Fujikura 2008); Ottawa sand (Fleshman and Rice 2014) and crushed sand (Cote et al. 2011).

Fig. 3 Hydraulic conductivity of different materials by experimental and KC methods: a) current study; b) compared to previous granular soils

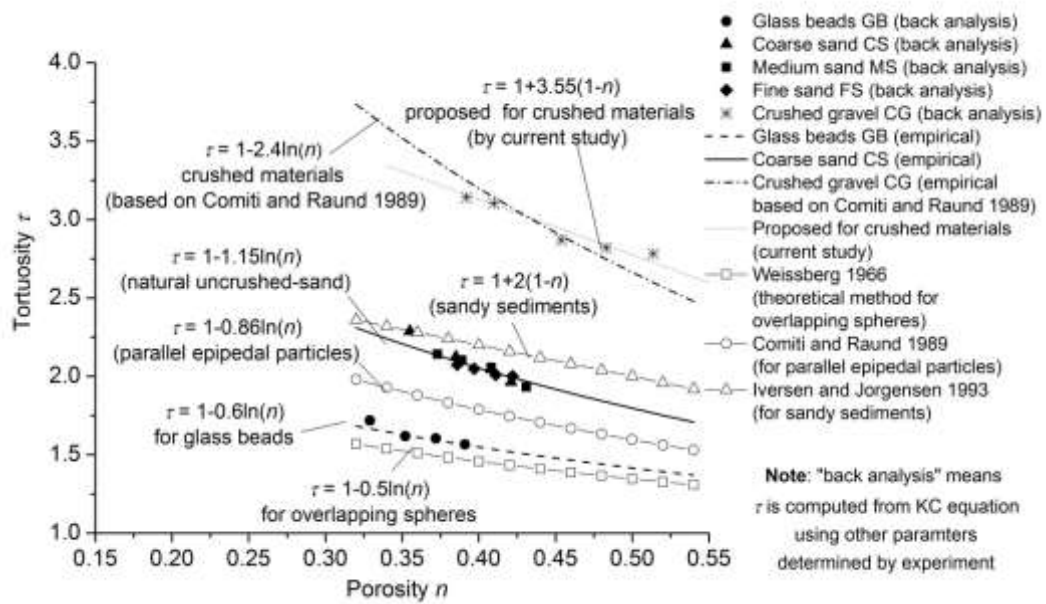


Fig. 4 Tortuosity of fluid flow through different shaped materials in comparison with previous studies